

# Experimental and Numerical Study on the Effects of Oxygen Methane Flames with Water Dilution for Different Pressures

J. P. Chica Cano, G. Cabot, S. de Persis, F. Foucher

**Abstract**—Among all possibilities to combat global warming, CO<sub>2</sub> capture and sequestration (CCS) is presented as a great alternative to reduce greenhouse gas (GHG) emission. Several strategies for CCS from industrial and power plants are being considered. The concept of combined oxy-fuel combustion has been the most alternative solution. Nevertheless, due to the high cost of pure O<sub>2</sub> production, additional ways recently emerged. In this paper, an innovative combustion process for a gas turbine cycle was studied: it was composed of methane combustion with oxygen enhanced air (OEA), exhaust gas recirculation (EGR) and H<sub>2</sub>O issuing from STIG (Steam Injection Gas Turbine), and the CO<sub>2</sub> capture was realized by membrane separator. The effect on this combustion process was emphasized, and it was shown that a study of the influence of H<sub>2</sub>O dilution on the combustion parameters by experimental and numerical approaches had to be carried out. As a consequence, the laminar burning velocities measurements were performed in a stainless steel spherical combustion from atmospheric pressure to high pressure (up to 0.5 MPa), at 473 K for an equivalence ratio at 1. These experimental results were satisfactorily compared with Chemical Workbench v.4.1 package in conjunction with GRIMech 3.0 reaction mechanism. The good correlations so obtained between experimental and calculated flame speed velocities showed the validity of the GRIMech 3.0 mechanism in this domain of combustion: high H<sub>2</sub>O dilution, low N<sub>2</sub>, medium pressure. Finally, good estimations of flame speed and pollutant emissions were determined in other conditions compatible with real gas turbine. In particular, mixtures (composed of CH<sub>4</sub>/O<sub>2</sub>/N<sub>2</sub>/H<sub>2</sub>O/ or CO<sub>2</sub>) leading to the same adiabatic temperature were investigated. Influences of oxygen enrichment and H<sub>2</sub>O dilution (compared to CO<sub>2</sub>) were disused.

**Keywords**—CO<sub>2</sub> capture, oxygen enrichment, water dilution, laminar burning velocity, pollutants emissions.

## I. INTRODUCTION

CARBON capture and storage (CCS) is presented as one of the most strategic solutions for GHG emission mitigation [1]. This process might be applied to high CO<sub>2</sub> emitters such as power plants, in which capture, transport and sequestration costs can be minimized.

J. P. Chica Cano is with the CORIA CNRS UMR 6614, University of Normandy, Rouen, France (phone: +33 2 32 95 97 33; fax: +33 2 32 95 97 80; e-mail: chicacaj@coria.fr).

G. Cabot is with the CORIA CNRS UMR 6614, University of Normandy, Rouen, France (phone: +33 2 32 95 97 6789; fax: +33 2 32 95 97 80; e-mail: cabot@coria.fr).

S. de Persis is with the ICARE CNRS UPER 3021, University of Orleans, Orleans, France (phone: +33 2.38.25.54.88; fax: +33 2.38.69.60.04; e-mail: depersis@cnrs-orleans.fr).

F. Foucher is with the PRISME, University of Orleans, Orleans, France (phone: +33 2 38 49 43 68; e-mail: fabrice.foucher@univ-orleans.fr).

Several CO<sub>2</sub> capture technologies exist [2]. Post combustion CO<sub>2</sub> capture process using a membrane separator is a promising and relatively efficient candidate, but its efficiency becomes interesting only if the CO<sub>2</sub> concentration in the exhaust gases exceeds 30% [3]. Normally, in traditional combustion process (e.g. in gas turbine), diluted exhaust gases contain no more than 5% of CO<sub>2</sub> due to the combustion products are mixing in air [4]. OEA as oxidant (higher than 21%) is exhibited as a possible way to reach the required CO<sub>2</sub> concentration in the exhaust gas. Nevertheless, it is mandatory to control its production to avoid an excess, due to its cost [5]. Consequently, the OEA production induces increases in the flame temperature, making it necessary to cool the flame and combustion chamber. This cooling can be achieved by EGR and/or by Steam Injection (SI). Coupling capture by membrane with OEA/EGR/SI (represented by CO<sub>2</sub> and H<sub>2</sub>O dilution) combustion is an unconventional process that must be studied, since it modifies drastically the combustion parameters even if the fuel is the same, methane. In order to analyze this novel process, it is important to understand the consequences of CO<sub>2</sub> and H<sub>2</sub>O dilution, as well as O<sub>2</sub> enrichment on fundamentals combustion parameters: ignition delay, flame speed and flame temperature. For this reason, this study is focused on the laminar flame velocities of CH<sub>4</sub>/O<sub>2</sub>/N<sub>2</sub>/H<sub>2</sub>O mixtures.

There are a huge number of studies in the literature which focus on understanding the effects of oxygen enrichment and/or CO<sub>2</sub> dilution on methane laminar premixed flames [6]-[9]. However, only a reduced number of fundamental flame speed studies of methane with H<sub>2</sub>O dilution have been reported. Measurements performed on conical flames were described in [10]-[12] and on outwardly expanding flames in [13], [14].

The effect of pressure on laminar methane flames diluted with water was studied for the first time, in 1971, by Babkin and V'Yun [13]. Their experimental device consisted of a spherical bomb that enabled the pressure to be varied from 0.1 to 7.0 MPa. In their study, they concluded that, for a given water content, the barometric exponent in the dependence of this velocity-pressure ( $S_U \sim P^n$ ) decreased as the pressure rose. They also found that a higher water content corresponded to a greater reduction in the exponent.

In 2009, Mazas et al. [10] studied the effect of O<sub>2</sub> enrichment in steam diluted methane flames but only at atmospheric pressure. In their experiments, performed in an axisymmetric burner, the O<sub>2</sub> percentage in the oxidant was varied from 0.21 - air - to 1.0 - oxycombustion, the

equivalence ratio from 0.8 to 1.6, and the steam dilution (in terms of water mole fraction in the reactants) from 0 to 0.5. They observed that the laminar burning velocity decrease was quasi-linear with increasing steam molar fraction, especially for highly oxygen-enriched flames.

In 2011, Galmiche et al. [14] compared the effects of different diluents ( $N_2$ ,  $CO_2$  and  $H_2O$ ) on laminar burning velocity at atmospheric pressure. They showed that  $CO_2$  dilution had a greater influence than  $H_2O$  dilution, due to its molar heat capacity.

In 2013, Albin et al. [12] studied the effect of steam dilution on laminar and turbulent methane/air flames at atmospheric pressure and for two different burners: Bunsen and V-flames. They concluded that a methane–air flame in ultra-wet conditions could be more than three times slower than a dry flame. This literature review shows that most of the available data are for atmospheric pressure, but few data are available at high pressure, which is the pressure used in most combustion applications. This study therefore aims at completing the experimental database by focusing on measurements of laminar flame velocities of  $CH_4/O_2/N_2/H_2O$  mixtures from 0.1 MPa to 0.5 MPa. The inlet temperature was fixed at 473 K and the equivalence ratio,  $\phi = [X(CH_4)/X(O_2)]/[X(CH_4)/X(O_2)]_s$ , where subscript  $s$  means stoichiometry, was fixed at 1 because the production cost of OEA and its production mode become a problem in the economic and environmental efficiency of a combustion process. To reduce this, it is necessary to burn with the minimum sufficient oxidant flow (in this case stoichiometric conditions). The dilution ratio,  $D.R = X(N_2)/X(O_2)$ , was set at 3.78 for air, and was varied as a function of oxygen enrichment, defined by the ratio  $\Omega = X(O_2)/[X(O_2) + X(N_2)]$ . The oxygen enrichment ratios ( $\Omega$ ) chosen were  $\Omega = 0.3, 0.5, 0.7, \text{ and } 1.00$ .

The setup used here is a spherical combustion chamber coupled with shadowgraphy. The parameters studied in this work are:

- The oxygen-enrichment ratio in the oxidizer  $\Omega = X(O_2)/[X(O_2) + X(N_2)]$ , which was varied from 0.21 (air) to 1.0 (pure oxygen);
- The  $H_2O$  mole fraction,  $X(H_2O)$ , in the mixture that was varied from 0 (dry conditions) up to the flame ignition limit for each condition (up to 20% under atmospheric pressure and up to 80% for  $\Omega = 0.5$ ).

- The pressure, which was varied from 0.1 to 0.5 MPa.

Calculations were performed using the Chemical Workbench v.4.1. Package [15] together with GRIMech3.0 [16] and comparisons with experiments conducted in the present study and taken from the literature were done. After validating the reaction mechanism, it was used to extrapolate results to higher pressure values, closer to gas turbine conditions. The specific objectives of the present work were thus to investigate the effects of oxygen enrichment and  $H_2O$  dilution on laminar methane flames at high pressure. For that purpose, measurements and calculations were compared and are discussed as a function of oxygen enrichment,  $H_2O$  dilution, and pressure.

## II. MODELLING

Thermodynamic and kinetic simulations were performed with the Chemical Workbench software package (CWB) [15] and the GRIMech3.0 mechanism [16].

Equilibrium calculations in isobaric and adiabatic conditions were carried out with CWB together with GRIMech3.0 to compute:

- The density of burnt  $\rho_b$  and unburnt  $\rho_u$  gases required by the experimental analysis;
- Adiabatic flame temperatures.

GRIMech3.0 [16], containing 53 species and 325 reversible reactions, was employed because it is a reference mechanism for the combustion of natural gas.

CWB was also used to compute unstretched laminar flame velocities. This code allows the calculation of flame velocity, temperature profiles and species mole fraction profiles in premixed laminar flames by solving for steady, isobaric and 1-dimensional flame propagation equations for continuity, energy, species and state. The present calculations were performed for freely propagating flames including multi-component and thermal diffusion effects. The flame model uses a high-order spatial discretization scheme and an adaptive mesh. It is important to note that a comparison between CWB and PREMIX code [17] was carried out (not presented here). The same result was obtained with CWB as with PREMIX using adaptive mesh parameters GRAD and CURV reduced to 0.001.

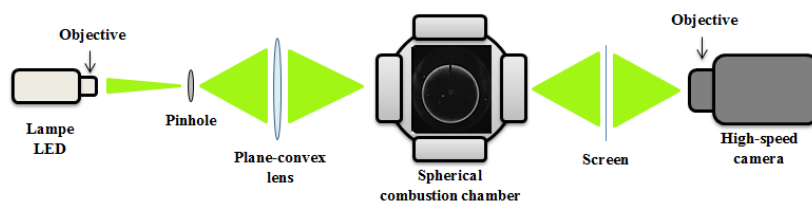


Fig. 1 Scheme of the experimental setup

## III. EXPERIMENTAL SET-UP AND METHODOLOGY

The device used here shown in Fig. 1 [14] consists of a stainless steel spherical combustion chamber with an inner diameter of 200 mm for a total volume of 4.2 L. The sphere is

surrounded by a resistance wire that can heat the sphere up to 473 K. A vacuum pump reduces the residual pressure inside the device to  $<0.003$  mbar before gas injection. Due to the oxygen enrichment, oxygen and nitrogen were added to get

the appropriate  $\Omega$  from 0.21 (air composition) to 1.0 (pure oxygen). The methane was introduced at the same time and was matched to the desired equivalence ratio. The gases were introduced via thermal flow meters (Brooks 5850S, 4 NL/min for nitrogen, 1.2 NL/min for oxygen and 0.5 NL/min for methane). The air/water injection was directed to the exit of the Coriolis flow controller (Bronkhorst mini CORI-FLOW 30 g/h) to convey the injected liquid. The inlet valve of the water/gas mixture and the capillary from this inlet valve and the vessel were heated to 473 K to ensure water vaporization. A fan installed inside the chamber ensured a perfectly homogeneous premixed mixture. The fan was stopped 5 s before ignition to avoid perturbations during flame propagation. A piezo-electric pressure transducer and a type-K thermocouple were used to check respectively the pressure level and the initial temperature before ignition. The maximum deviation between the effective initial pressure inside the combustion chamber and the required initial pressure was about 1%. The initial temperature of the prepared mixture was known at 2 K. Two tungsten electrodes (diameter 1 mm), with a 1-mm gap, linked to a conventional capacitive discharge ignition system, were used for spark production in the center of the chamber. Four transparent windows (diameter 82 mm) provided optical access to the chamber. A LED illuminator (HardSoft DLR IL104G) equipped with an objective (HSO-PL-360) was used to provide continuous and incoherent light with a wavelength of 528 nm. A parallel light was created using a pinhole (diameter 3 mm), placed at the focal point of the objective, and a plane-convex lens (diameter 70 mm, focal length 1000 mm). After passing through the lens and the combustion chamber, the beam is displayed on a screen. Visualization of the flame was obtained using a classical shadowgraph method. Fig. 2 shows instantaneous images recorded using a high-speed video camera (Photron Fastcam SA5) operating at from 6000 to 20000 images per second.

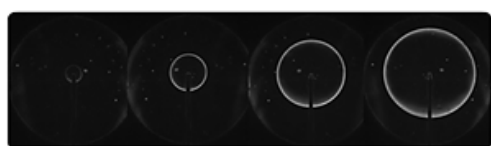


Fig. 2 Spherical flame propagation, for 0.5 MPa,  $\Omega=1.0$ ,  $X(\text{H}_2\text{O})=0.65$ ,  $T_0=473$  K,  $\Phi=1$ , in which the flame is propagated normally

The acquisition frequency was adjusted as a function of the increase in the flame speed displacement to ensure that the flame propagation was described by enough images (at least 20), and the resolution was  $512 \times 512$  pixels<sup>2</sup>.

Measurements were limited to flames with diameters <50mm, corresponding to a volume of burned gases less than 1.6% of the chamber volume [18]. Under such conditions, the total chamber pressure can be considered constant during the initial stage of flame expansion. The temporal evolution of the expanding spherical flame was then analyzed and coupled to the non-linear methodology [19], [20]. This methodology is

based on the nonlinear equation proposed by Kelley et al. [21]:

$$\left(\frac{s_b}{s_b^0}\right) 2 \ln \left(\frac{s_b}{s_b^0}\right) = -\frac{L_b k}{s_b^0} \quad (1)$$

The stretch rate ( $k$ ), (2), is defined as the temporal rate of change of a flame surface element of area  $A$ :

$$k = \frac{1}{A} \left(\frac{dA}{dt}\right) \quad (2)$$

In the case of a spherically expanding laminar flame, the total stretch acting on the flame is defined as (3):

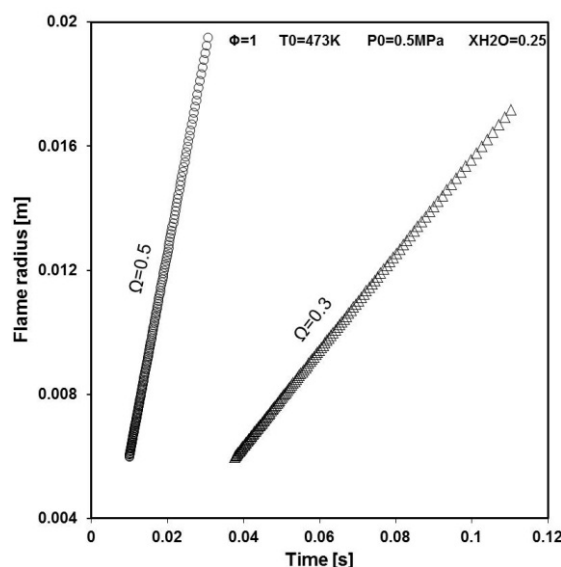


Fig. 3 Flame front radius in m, as a function of time in s, for  $\Omega=0.3$  and  $0.5$ ,  $\Omega=1$ ,  $X\text{H}_2\text{O}=0.25$  and  $P=0.5$  MPa

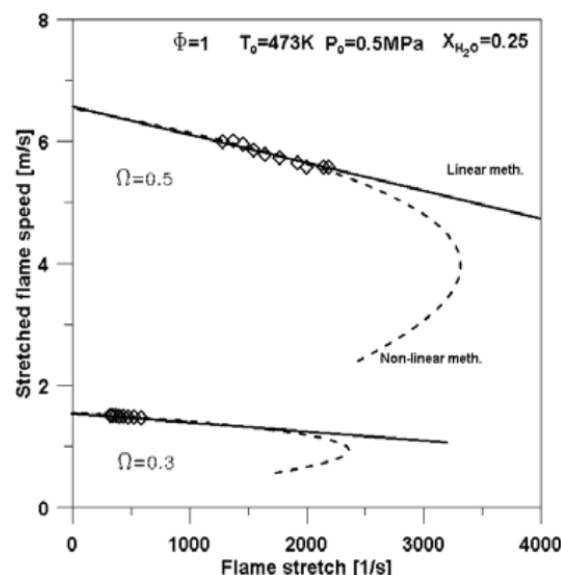


Fig. 4 Stretched flame speed in m/s as a function of flame stretch (in  $\text{s}^{-1}$ ) for  $\Omega=0.3$  and  $0.5$ ,  $\Omega=1$ ,  $X\text{H}_2\text{O}=0.25$  and  $P=0.5$  MPa. Symbol: experimental velocity as a function of flame stretch, dashed line: nonlinear methodology, solid line: linear extrapolation methodology

$$k = \frac{2}{R_f} \left( \frac{dR_f}{dt} \right) \quad (3)$$

where  $R_f$  is the flame front radius. Fig. 3 shows the experimental measures of the influence of oxygen enrichment ( $\Omega$ ) on this radius  $R_f$  as a function of time, for two conditions: circles correspond to  $\Omega=0.5$  and the triangles ones to  $\Omega=0.3$ . In this case, the oxygen increase explains the rapid evolution of the flame front radius for  $\Omega=0.5$  with respect to  $\Omega=0.3$ .

During this temporal evolution, the flame front is affected by the stretch rate. Fig. 4 shows the experimental measurements (diamonds) of the stretched flame speed ( $S_b$ ) as a function of the flame stretch ( $K$ ) for two reactive mixture conditions. The solid line represents the linear correlation, and the dashed line represents the non-linear correlation from which the unstretched propagation flame velocity  $S_b^0$  is extrapolated for  $k = 0$ .

In the experimental conditions shown in Fig. 4, one can observe that the linear methodology (solid line) and non-linear methodology give the same result for  $S_b^0$ . This can be explained, as shown in Fig. 5, by low values of the Markstein length whatever the air enrichment ( $\Omega$ ) which involves the no dependency of the mixture on stretch. The real benefit of the non-linear equation is only observed when the Markstein length reaches or exceeds 1 mm principally under fuel-lean conditions when the Lewis is higher than the unity.

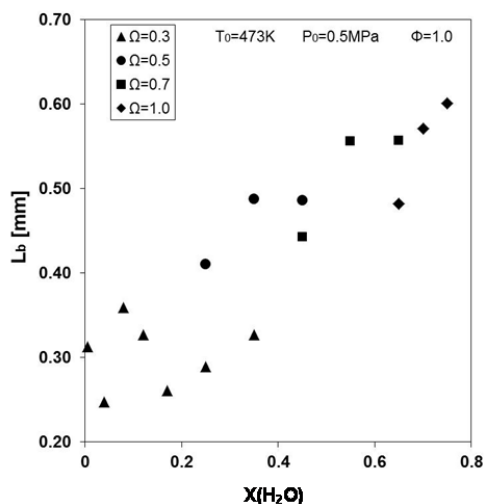


Fig. 5 Experimental Markstein lengths,  $L_b$  in mm, as a function of  $H_2O$  dilution, for:  $P_0=0.5$  MPa,  $\Phi=1$  and  $T_0=473$  K. Varying  $\Omega$

The fundamental laminar burning velocity  $S_L^0$  is finally obtained by taking into account the effects of the expansion factor:

$$\frac{S_b^0}{S_L^0} = \frac{\rho_u}{\rho_b} \quad (4)$$

where  $\rho_u$  and  $\rho_b$  are respectively the density ratios of unburned and burned gases. Assuming kinetic equilibrium, this ratio was estimated thanks to CWB coupled with GRIMEch3.0 in isobaric and adiabatic conditions.

## IV. RESULTS AND DISCUSSION

### A. Effect of $H_2O$ Dilution on Methane/Air Flames Varying Initial Pressure and Temperature

Fig. 6 shows the effect of the initial temperature on the fundamental laminar burning velocity  $S_L^0$  in  $cm.s^{-1}$ . The equivalence ratio was kept constant at stoichiometric value ( $\Phi=1$ ). The experimental results obtained in this work at  $T_0=300$  K (for  $X(H_2O)=0$ ), at  $T_0=393$  K and  $T_0=473$  K as a function of  $H_2O$  mole fraction are plotted and compared to calculations obtained with CWB and experimental results taken from the literature: Galmiche et al. [14] at  $T_0=393$ K, Boushaki et al. [11] at  $T_0=300$  K, Babkin and V'Yun [13] at  $T_0=400$  K, Albin et al. [12] at  $T_0 = 480$  K, and Mazas et al. [10] at  $T_0=473$  K.

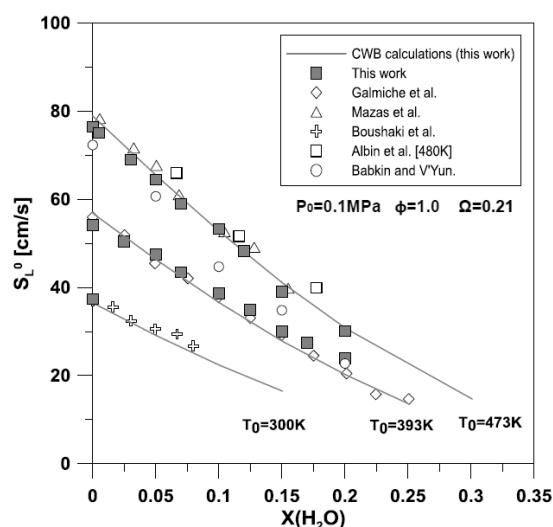


Fig. 6 Laminar burning velocities as a function of  $H_2O$  dilution, for three different initial temperatures: 300 K, 393 K, 473 K. ( $P_0=0.1$  MPa)

As expected, whatever the initial temperature, fundamental laminar burning velocities,  $S_L^0$  expressed in  $cm.s^{-1}$ , decrease when the water mole fraction increases. For a given water mole fraction, the fundamental laminar burning velocity increases with initial temperature. For instance, for  $T_0=473$  K, the fundamental laminar burning velocity decreases with the  $H_2O$  mole fraction, from about 80  $cm/s$  in dry conditions down to about 30  $cm/s$  in wet conditions ( $X(H_2O)=0.20$ ). This trend is shown by experimental data and is perfectly reproduced by calculations. It is important to note that our experimental results are in good agreement with experimental data taken from Mazas et al. [10]. The experimental results of Babkin and V'Yun [13] are the lowest. Whatever the temperature, there is a good agreement between our results and calculations and the experimental data from the literature except those of Albin et al. [12] which seem to be too high, but the authors mentioned some experimental difficulties (stability limitation for Bunsen flames especially for lean and wet conditions, reduced for the highest temperature). The results presented here show a very good agreement between our experiments and modelling. This result allows us to consider that the

experimental device is validated in the case of water dilution under atmospheric pressure. It is thus possible to use it to measure laminar flame velocities at high pressure.

Fig. 7 shows the comparison between experimental and calculated fundamental laminar burning velocities,  $S_L^0$  in  $\text{cm}\cdot\text{s}^{-1}$ , as a function of pressure (from 0.1 to 0.5 MPa) and  $\text{H}_2\text{O}$  dilution (for  $X(\text{H}_2\text{O})$  ranges from 0 to 0.20) for an equivalence ratio  $\Phi=1$  and an initial temperature  $T_0 = 473$  K. For comparison, experimental results from Babkin and V'Yun [13] are also plotted. Experimental and numerical results show that for a given water mole fraction, the fundamental laminar burning velocity,  $S_L^0$  in  $\text{cm}\cdot\text{s}^{-1}$ , decreases with increasing pressure: from about 80  $\text{cm/s}$  in dry conditions under atmospheric pressure down to about 45  $\text{cm/s}$  at high pressure (0.5 MPa); from about 30  $\text{cm/s}$  for a water mole fraction of 20% under atmospheric pressure down to about 15  $\text{cm/s}$  at high pressure (0.5 MPa).

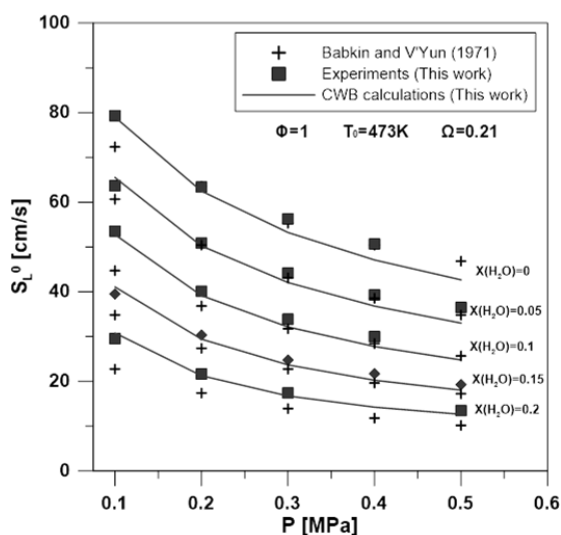


Fig. 7 Laminar burning velocities as a function of initial pressure in MPa, for different  $\text{H}_2\text{O}$  dilution: from 0 to 0.2 ( $T_0=473$  K)

For a given pressure, the fundamental laminar burning velocity,  $S_L^0$  in  $\text{cm}\cdot\text{s}^{-1}$ , decreases with water dilution,  $X(\text{H}_2\text{O})$ . The agreement between our experimental results and those of Babkin and V'Yun [13] are better for low  $\text{H}_2\text{O}$  dilution and higher pressure. Modelling obtained with CWB and GRIMEch3.0 is in good agreement with our experimental results.

### B. Effect of $\text{H}_2\text{O}$ Dilution and High Pressure on Methane Oxygen-Enriched Flames

#### 1) Global Thermal Properties

One of the objectives of this work is to observe and compare experimental and numerically, the evolution of methane/oxygen enriched flames in  $\text{H}_2\text{O}$  dilution conditions at high temperatures and pressures. For this reason, Fig. 8 illustrates the influence of the  $\text{O}_2$  enrichment in the flame temperature profile to conditions ( $P_0=0.5$  MPa,  $T_0=473$  K and  $\Phi=1.0$ ) that were evaluated in the same experimental way. As expected, the mixture with the highest amount of oxygen has

the highest inclination and the highest temperature peak with respect to the others. This is due to the increase of oxygen that encourages acceleration of fuel oxidation, being reflected in the temperature profile. From this evolution, the temperature gradient is found, which announces the reaction with a higher rate of heat release.

Consequently, Fig. 9 shows the temperature gradient for similar flame conditions. The temperature gradient is coherent with the flame temperature, placing the oxy-methane flame with a higher peak. This increase in oxygen is the main agent in the increase of the rate of heat release, which indicates an accelerated reaction process.

With respect to these results, Fig. 10 shows the laminar flame thickness following the classic formulation (5) [22]. Laminar flame thickness is an important thermal parameter to suggest the overall rate of flame reaction.

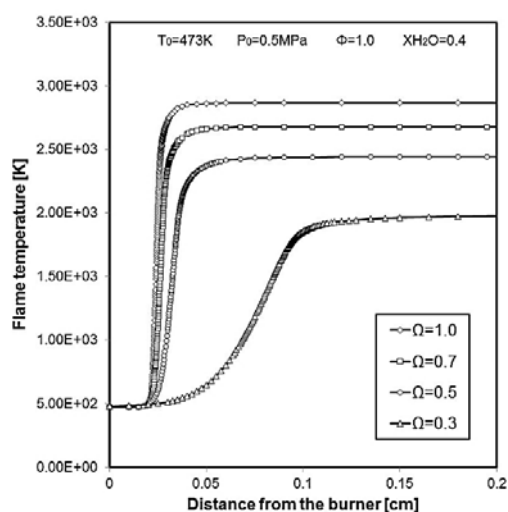


Fig. 8 Flame temperature profiles for stoichiometry methane/oxygen enriched flames with  $\text{H}_2\text{O}$  dilution. ( $\Omega$  from 0.3 to 1.0,  $T_0=473$  K,  $P_0=0.5$  MPa,  $X(\text{H}_2\text{O})=0.4$ )

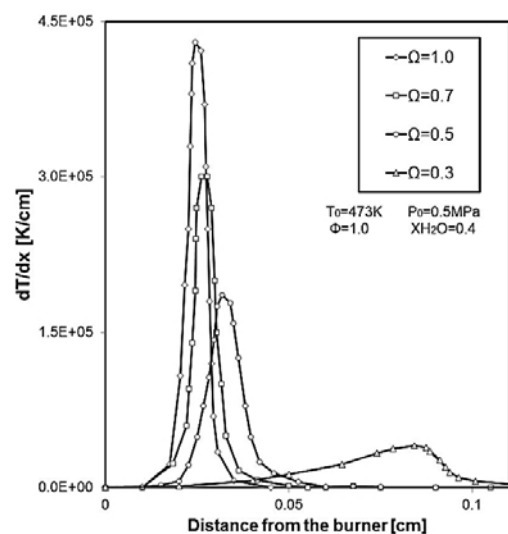


Fig. 9 Temperature gradients for stoichiometry methane/oxygen enriched flames with  $\text{H}_2\text{O}$  dilution. ( $\Omega$  from 0.3 to 1.0,  $T_0=473$  K,  $P_0=0.5$  MPa,  $X(\text{H}_2\text{O})=0.4$ )

$$\delta_F = \frac{T_{max} - T_0}{(dT/dx)_{max}} \quad (5)$$

where  $T_{max}$  is the adiabatic flame temperature,  $T_0$  is the unburned gas temperature, and  $(dT/dx)_{max}$  is the maximum slope of the temperature profile. The  $(dT/dx)_{max}$  is found using the premixed flame code: CWB [15] together with GRIMEch3.0 [16] is used. In order to explain the influence of oxygen enrichment and water dilution, the flame thickness was evaluated. This parameter has a strong impact on the hydrodynamic instabilities of the flame. For our case, where the experimental flame is spherical, the flame thickness has an important influence on the stretching of the flame front, which is a leading parameter to control the cellularity of the flame and the curvature. In this way, it is possible to conclude that in the experimental cases where flame instabilities were presented (e.g. cellularity), it was due to a decrease in the flame thickness (i.e. increase of oxygen enrichment and little dilution of water) and the curvature became weaker.

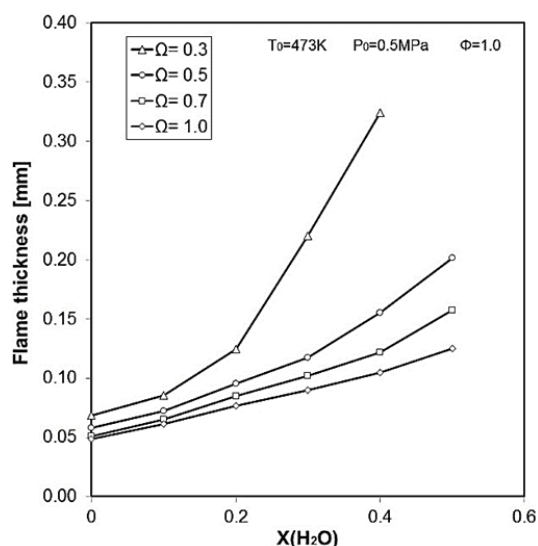


Fig. 10 Laminar flame thickness for stoichiometry methane/oxygen enriched flames. ( $\Omega$  from 0.3 to 1.0,  $T_0=473$  K,  $P_0=0.5$  MPa)

It is clear that the enrichment of oxygen leads to reduce the flame thickness, and this is controlled by increasing the  $H_2O$  dilution on the flame.

### 2) On Laminar Burning Velocity

The effect of water dilution,  $X(H_2O)$ , and oxygen-enrichment,  $\Omega$ , on the fundamental laminar burning velocity,  $S_L^0$  in  $cm.s^{-1}$ , of stoichiometric methane flames was investigated at high pressure for an initial temperature  $T_0=473$  K. Fig. 11 shows the experimental and numerical data obtained in the following conditions:  $\Omega = 0.3, 0.5, 0.7$  and  $1$ ;  $P_0 = 0.5$  MPa and  $X(H_2O) = 0$  to  $0.8$ .

As expected, Fig. 11 shows that for a given  $H_2O$  dilution, the fundamental laminar burning velocity,  $S_L^0$  in  $cm.s^{-1}$ , increases as a function of oxygen-enrichment,  $\Omega$ . In dry conditions, the laminar flame velocity is about  $100$   $cm/s$  for  $\Omega=0.3$  and increases up to about  $470$   $cm/s$  in oxycombustion

conditions. However, for a given oxygen-enrichment, the laminar flame velocity decreases when  $H_2O$  dilution increases. Increasing the water content in the mixture not only decreases the laminar flame velocity but also decreases the flame temperature, which directly affects the thermal diffusivity. Additionally, the fuel content will be replaced by the increase in the oxygen content and the dilution of water and, in turn, the energy content in the mixture will also be reduced.

Calculations obtained with CWB and GRIMEch3.0 are in excellent agreement with experimental values, even if the experimental values are always slightly higher than those of the simulations. These results validate the GRIMEch3.0 mechanism in this domain of oxygen enrichment and  $H_2O$  dilution, demonstrating its reliability for calculations at higher pressure and temperature conditions that cannot be achieved in a laboratory experimental setup.

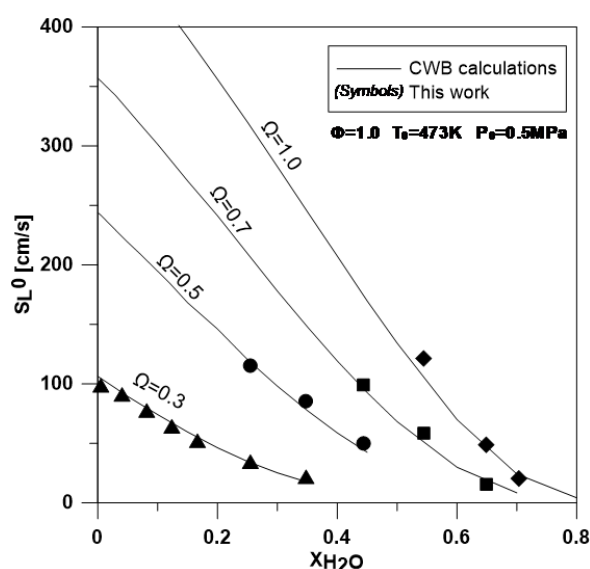


Fig. 11 Comparison between experimental (our results: symbols) and calculated (with CWB and GRIMEch3.0, solid lines) fundamental laminar burning velocities,  $S_L^0$ , in  $cm.s^{-1}$ , as a function of  $H_2O$  dilution,  $X(H_2O)$ , for a pressure  $P_0=0.5$  MPa,  $\phi=1$  and  $T_0=473$  K

The laminar burning velocity is a criterion used to predict the flame structure. In the combustion chamber, the flame has to be compact and especially stable. Moreover, in the case of premixed flame, the flame velocity is a good criterion to predict flashback phenomena.

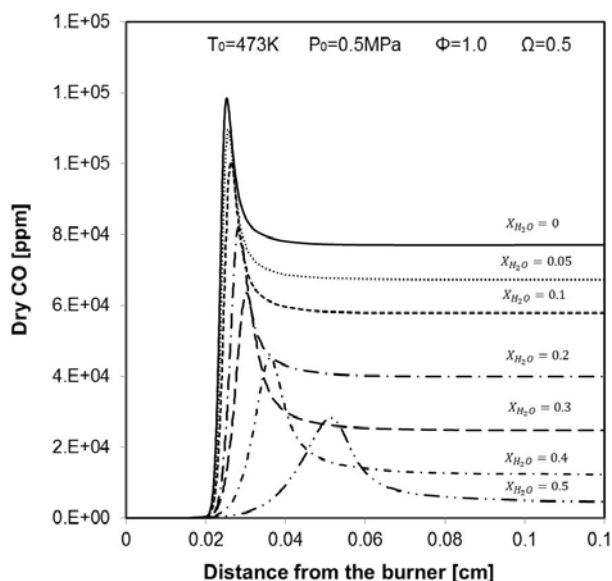
### 3) On CO and NO Emissions

In order to understand the effect of  $H_2O$  dilution and  $O_2$  enrichment on pollutant emissions, Fig. 12 (a) for CO emissions and Fig. 12 (b) for NO emissions, are plotted. It is possible to plot NO and CO mole fractions in ppm dry conditions, with the help of CWB together with GRIMEch3.0 in a freely propagating flame as a function of the distance from the burner. In this option, the energy equation is solved assuming an adiabatic system; the value obtained for the highest distance corresponds to thermodynamic equilibrium.

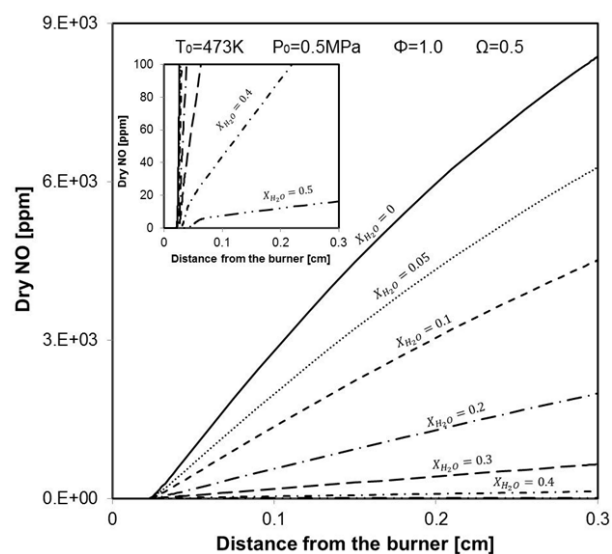
The modelling conditions for CO and NO mole fraction in

ppm dry conditions profiles are chosen from the experiments evaluated above: important O<sub>2</sub> enrichment to allow large dilution rates. X(H<sub>2</sub>O) from 0 to 0.5, Ω=0.5, P<sub>0</sub>=0.5 MPa, T<sub>0</sub>=473 K.

Under specific combustion conditions, the CO concentration in the exhaust gases is determined during the oxidation of the fuel and consumed normally by reaction: CO+OH=CO<sub>2</sub>+H. However, the presence of diluents such as H<sub>2</sub>O can play an important role in the production of these radicals (O and H), which in turn, increases or decreases the production of polluting emissions.



(a)



(b)

Fig. 12 Calculated dry CO and NO mole fractions (in ppm) as a function of the distance from the burner (cm) for different H<sub>2</sub>O dilution: from 0 to 0.5. CWB with FREE option in conjunction with GRIMech3.0 was used. (T<sub>0</sub>=473 K, P<sub>0</sub>=0.5 MPa, Ω=0.5, Φ=1.0)

In the case of this study, Fig 12 (a) shows that the dilution of water has a positive effect on the reduction of CO concentration in exhaust gases, depending on the amount of diluted water, which reduces the flame temperature via radical formation OH through H<sub>2</sub>O+H=OH+H<sub>2</sub> [23], [24]. On the other hand, Fig. 12 (b) shows a significant reduction of NO emissions, from the case without dilution of water X(H<sub>2</sub>O)=0, to the case with dilution X(H<sub>2</sub>O)=0.50. This is mainly due to thermal effects, dilution and reduction of N<sub>2</sub> concentration. The decreases in both the adiabatic flame temperature and the flame velocity, thanks to the increase in the percentage of water dilution, are some of the main keys put in place to reduce the NO emissions in the gas turbine [25], [26]

With these results shown in Figs. 12 (a) and (b), it is clear to observe the positive effect that dilution of water has on pollutant emissions: reduction of CO/NO emissions. Nevertheless, it is important to note the care that must be taken at the adiabatic flame temperature and flame speed, to avoid extinction and/or flame instabilities.

## V. CONCLUSION

In this paper, the effect of H<sub>2</sub>O dilution in oxy methane flames was studied experimental and numerically. Measurements were performed using the shadowgraph technique in a spherical combustion chamber at atmospheric and high pressure (0.5 MPa) for preheated gas mixtures (T<sub>0</sub>=473 K). The ratio Ω=X(O<sub>2</sub>)/[X(O<sub>2</sub>)+X(N<sub>2</sub>)] was varied from 0.21 (air) to 1.0 (pure oxygen) and the H<sub>2</sub>O mole fraction in the mixture, X(H<sub>2</sub>O), was varied from 0 to 0.8 (flame extinction), for an equivalence ratio fixed at 1. Experimental results were satisfactorily compared with experimental data taken from the literature when available as well as with calculations obtained using CWB [15] and PREMIX code [17] in conjunction with the GRIMech3.0 mechanism [16]. Under atmospheric pressure, the effect of water dilution on methane/air flames as a function of the initial temperature was studied. At high pressure, a novel study of the effect of water dilution and oxygen-enrichment on global thermal properties, on laminar flame velocities and emissions was performed.

The present study is a preliminary investigation as the final aim of our work is to compare NO and CO emissions predicted by a gas turbine network coupled with a detailed reaction mechanism to measurements carried out in a reference gas turbine. Thanks to the present work, the gas turbine conditions were determined and the reaction mechanism was validated. Furthermore, this preliminary study is of great interest from a combustion point of view because:

- It contributes to the extension of the experimental database on CH<sub>4</sub>/O<sub>2</sub>/N<sub>2</sub>/H<sub>2</sub>O laminar flame velocities at high pressure in air and oxygen-enriched conditions.
- It elucidates the effect of H<sub>2</sub>O dilution and oxygen enrichment on the flame behavior.

## ACKNOWLEDGMENT

The research leading to these results received funding from the COCC program in France through the support of the

EMC3Labex and Caprysses Labex.

REFERENCES

- [1] Herzog H. What future for carbon capture and sequestration. *Environ Sci Tech*2001; 35(7): 148-53.
- [2] Davidson O, Metz B. Special report on carbon dioxide capture and storage. Geneva, Switzerland: International Panel on Climate Change, www.ipcc.ch; 2005.
- [3] Belaisaoui B, Cabot G, Cabot MS, Willson D, Favre E. An energetic analysis of CO<sub>2</sub> capture on a gas turbine combining flue gas recirculation and membrane separation. *Energy* 2012; 38: 167-75.
- [4] Favre E, Bounaceur R, Roizard D. A hybrid process combining oxygen enriched air combustion and membrane separation for postcombustion carbon dioxide capture. *Separ Purif Technol* 2009; 68:30-6.
- [5] Yang H, Xu Z, Fan M, Gupta R, Slimane RB, Bland AE, Wright I. Progress in carbon dioxide separation and capture: a review. *Journal of Environmental Sciences* 2008; 20:14-27.
- [6] Khan AR, Anbusarayanan S, Kalathi L, Velamat R, Prathap C. Investigation of dilution effect with N<sub>2</sub>/CO<sub>2</sub> on laminar burning velocity of premixed methane/oxygen mixtures using freely expanding spherical flames. *Fuel* 2017; 196: 225-32.
- [7] Jourdaine P, Mirat C, Claudal J, Lo A, Shculler T. A comparison between the stabilization of premixed swirling CO<sub>2</sub>-diluted methane oxy-flames and methane/air flames. *Fuel* 2016; 201: 156-164. <http://dx.doi.org/10.1016/j.fuel.2016.11.017>.
- [8] Li YH, Chen GB, Lin YC, Chao YC. Effects of flue gas recirculation on the premixed oxy-methane flames in atmospheric condition. *Energy* 2015; 89: 845-57.
- [9] Hu X, Yu Q, Liu J, Sun N. Investigation of laminar flame speeds of CH<sub>4</sub>/O<sub>2</sub>/CO<sub>2</sub> mixtures at ordinary pressure and kinetic simulation. *Energy* 2014; 70: 626-34.
- [10] Mazas A, Fiorina B, Lacoste DA, Schuller T. Effects of water vapor addition on the laminar burning velocity of oxygen-enriched methane flames. *Combustion and Flame* 2011; 158: 2428-40.
- [11] Boushaki T, Dhué Y, Selle L, Ferret B, Poinot T. Effects of hydrogen and steam addition on laminar burning velocity of methane-air premixed flames: Experimental and numerical analysis. *International Journal of Hydrogen Energy* 2012; 37: 9412-2.
- [12] Albin E, Nawroth H, Göke S, D'Angelo Y, Paschereit CO. Experimental investigation of burning velocities of ultra-wet methane-air-steam mixtures. *Fuel Processing Technology* 2013; 107: 27-35.
- [13] Babkin VS and V'yun AV. Effect of water vapor on the normal burning velocity of a methane - air mixture at high pressures. *Combust Explo Shock Waves* 1971; 7(3): 339-41.
- [14] Galmiche B, Halter F, Foucher F, Dagaut P. Effects of dilution on laminar burning velocity of premixed methane/air flames. *Energy & Fuels* 2011; 25(3): 948-54.
- [15] Deminsky M, Chorko, V, Belov G, Cheshigin I, Knizhnik A, Shulakova E, Shulakov M, Iskan-darova I, Alexandrov V, Petrushev A, Kirillov I, Strelkova M, Umanski S, and Potapkin B. CWB. *Comput Mater Sci* 2003;28:169-78. <http://www.kintechlab.com/products/chemical-workbench>.
- [16] Smith GP, Golden DM, Frenklach M, Moriarty NW, Eiteneer B, Goldenberg M, Bowman CT, Hanson RK, Song S, Gardiner WC, Lissianski VV, Qin Z, GRI Mech 3.0 Mechanism (1999), [http://www.me.berkeley.edu/gri\\_mech/](http://www.me.berkeley.edu/gri_mech/).
- [17] Kee, R. J.; Grcar, J. F.; Smooke, M. D.; Miller, J. A. A Fortran Program for Modeling Steady Laminar One-Dimensional Premixed Flames, Sandia Technical Report SAND85-8240; Sandia National Laboratory: Albuquerque, NM, 1985.
- [18] Buckmaster J. Slowly varying laminar flames. *Combustion and Flame* 1977; 28: 225e39.
- [19] Tahtouh T, Halter F, Mounaïm-Rousselle C. Measurement of laminar burning speeds and Markstein lengths using a novel methodology. *Combustion and Flame* 2009; 156:1735-43.
- [20] Bradley D, Hicks R.A, Lawes M, Sheppard C.G.W, Woolley R. The measurements of laminar burning velocities and Markstein numbers for iso-octane-air and iso-octane-n-heptane-air mixtures at elevated temperatures and pressures in a explosion. *Combustion and Flame* 115: 126-144 (1998).
- [21] Kelley AP, Law CK. Nonlinear effects in the extraction of laminar flame speeds from expanding spherical flames. *Combust. Flame* 2009; 156:1844-51.
- [22] Hu G, Zhang S, Li QF, Pan XB, Liao SY, Wang HQ, et al. Experimental investigation of the effects of hydrogen addition on thermal characteristics of methane/air premixed flames. *Fuel* 2014;115:232-40.
- [23] Renard C, Musick M, Van Tiggelen P.J, Vandooren J. Effect of CO<sub>2</sub> or H<sub>2</sub>O addition on hydrocarbon intermediates in rich C<sub>2</sub>H<sub>4</sub>/O<sub>2</sub>/Ar flames. *Proc. European Combustion Meeting; Orleans, France, October 25-28, 2003*.
- [24] Le Cong T, Dagaut P, Dayma G. Oxidation of natural gas, natural gas/syngas mixtures and effect of burnt gas recirculation: Experimental and detailed kinetic modelin. *J. Eng. Gas Turbine Power* 2008, 130, 041502-1,10.
- [25] Chica Cano JP, Cabot G, Foucher F, De Persis S; *Fuel* 2017 (submitted); Effects of oxygen enrichment and water dilution on laminar methane flames at high pressure.
- [26] Pugh DG, Bowen PJ, Marsh R, Crayford AP, et al. Dissociative influence of H<sub>2</sub>O vapour/spray on lean blowoff and NO<sub>x</sub> reduction for heavily carbonaceous syngas swirling flames. *Combustion and Flame* 177: 37-48(2017).